
Article

Detecting Underwater Concrete Cracks with Machine Learning: A Clear Vision of a Murky Problem

Ugnė Orinaitė ¹ , Viltė Karaliūtė ¹, Mayur Pal ¹ * , Minvydas Ragulskis ¹ 

¹ Centre for Nonlinear Systems, Department of Mathematical Modelling, Kaunas University of Technology, 51368 Kaunas, Lithuania; ugne.orinaite@ktu.lt (U.O.); minvydas.ragulskis@ktu.lt (M.R.); mayur.pal@ktu.lt (M.P.); vilte.karaliute@ktu.edu (V. K.)

* Correspondence: mayur.pal@ktu.lt (M.P.)

Abstract: This paper presents the development of an underwater crack detection system for structural integrity assessment of submerged structures, like offshore oil and gas installations, underwater pipelines, underwater foundations for bridges, dams etc. Focus is on use of machine learning based approaches. First a detailed literature review of state of the current methods for underwater surface crack detection is presented highlighting challenges and opportunities. An overview of image augmentation approach for creation of underwater optical effects is also presented. Experimental results using standard network based machine learning approach, used for surface crack detection in onshore environment, is presented. Series of Test cases are presented where existing networks performance are improved using augmented images for underwater conditions. The effectiveness and accuracy of the proposed approach in detecting cracks in underwater concrete structures is demonstrated. The proposed approach has the potential to improve the safety and reliability of underwater structures and prevent catastrophic failures.

Keywords: Underwater; Crack detection; Machine learning; Transfer learning; Augmentation; Non-destructive testing; Safety; Reliability

1. Introduction

Underwater concrete structures serve various important purposes in different areas, including infrastructure projects, erosion and storm protection, support for offshore energy projects, and the creation of habitats for marine life. These structures are designed to provide stability, durability, and the ability to withstand harsh underwater environments. They play a crucial role in supporting infrastructure development while also protecting the environment and marine ecosystems. Ensuring the structural integrity of underwater concrete structures is of utmost importance to prevent catastrophic failures. The underwater environment poses unique challenges to the integrity of these structures, such as saltwater corrosion and the impact of waves, which can lead to cracks and other types of damage. It is vital to identify and monitor fractures in underwater concrete constructions to identify potential weaknesses and take corrective measures in a timely manner.

However, it is a challenging endeavor to identify and monitor fractures in underwater concrete constructions due to several factors. Limited visibility, difficult access, and harsh conditions make it difficult to visually inspect these structures. Therefore, reliable and efficient methods are needed to detect and monitor cracks in underwater environments. Some of the most often used methods for fracture identification and monitoring in underwater concrete structures are:

- Visual inspections by divers: Specially trained divers can perform visual inspections of the structures to identify visible cracks or signs of damage. However, this method is limited by the accessibility of the structure and the diver's ability to navigate and inspect the entire surface. Such inspections are also known for high risk for the divers involved in carrying out such inspections.

- Non-destructive testing techniques: Techniques such as ultrasonic testing and acoustic emission monitoring may be used to evaluate the interior condition of a concrete structure and detect cracks or other flaws. These methods rely on the analysis of sound waves or emitted signals to identify potential issues. However, they require specialized equipment and expertise to perform accurately. The time required for acquisition and processing of data is long. often cost of such data acquisitions are very high as well. 38
39
40
41
42
43
44
- Advanced technologies: Underwater drones and robots equipped with cameras and sensors are emerging as valuable tools for crack detection and monitoring. These autonomous or remotely operated devices can access hard-to-reach areas, capture high-resolution images or videos, and collect data on the condition of the structures. This technology offers improved accessibility and accuracy in crack detection. The technique presented in this paper is an addition to such a technology for underwater inspections. 45
46
47
48
49
50
51

In modern time the amount of underwater infrastructure has increased many folds, which includes internet cables, electric cables linked to offshore wind mills, and oil and gas pipe lines among other important infrastructure. Implementing reliable methods for detecting and monitoring cracks in underwater concrete structures is crucial for ensuring their long-term durability and safety. While significant research has been conducted on crack detection systems for onshore and above-water structures [1,2], less attention has been given to underwater crack detection. The work presented in this paper focuses specifically on addressing this gap and developing effective crack detection methods for underwater concrete structures. By improving our ability to detect and monitor cracks in underwater concrete structures, we can identify issues early, implement appropriate repairs or maintenance, and ensure the continued functionality and safety of these vital underwater assets. 52
53
54
55
56
57
58
59
60
61
62
63

The paper is structured as follows: An overview of different techniques used in underwater concrete crack detection is presented in section 2. Challenges of underwater concrete crack detection is discussed in section 3. Available methods to mitigate the challenges related to underwater crack detection system is discussed in section 4. Section 5 presents an overview of the data set used in this paper to demonstrate use of machine learning based approach for underwater crack detection. Machine learning based underwater crack detection system along with series of test cases is presented in section 6. Conclusions follows in section 7. 64
65
66
67
68
69
70
71

2. An overview of the techniques used for underwater concrete crack detection 72

2.1. Visual inspection: basic method for detecting cracks in underwater concrete, but limited by 73 water clarity and visibility 74

By quantifying the likelihood distribution of sea surface slopes, numerical approaches have enabled researchers to investigate both the refraction and reflection of light from the sky and the sun via roughened sea surfaces. In one study, the researchers explored various optical phenomena, such as the refracted sun's glitter, the brightness and reflectivity of an uneven sea surface owing to sky light and the reflection of a harsh sea surface from direct sunlight [3]. While research on cracks in underwater surfaces is limited, most studies focus on the effects of water on various chemicals, their resistance to the environment, or their impact on the environment [4–6]. 75
76
77
78
79
80
81
82

Researchers have studied shade on under-water optical radiometers employing Monte Carlo computations of a light field with both the presence and lack of the sensors to [7]. Optical sensors from space have been used to observe surface water, and various techniques have been developed to eliminate cloud or terrain shadows [8–12]. Additionally, flash photography directed vertically downward toward the water surface has been used to interpret wave slopes. Researchers have studied various optical effects of water, including optical absorption, temperature and humidity effects, dissolved organic materials, biolog- 83
84
85
86
87
88

ical vegetation interaction, pressure effects, and optical propagation in turbulent water [13–20]

2.2. Acoustic methods: use of sound waves to detect cracks, including impact-echo, impulse response, and ultrasonic methods. Fluorosensor.

In [21], it is described how optically and near-infrared wavelengths may be used to detect water depth and substrate type as two key factors in river physical habitat. The approach provided in [22] was used to remotely track chlorophyll content in fresh waterways and was shown to be strongly associated with real-world data, allowing for the detection of changes in surface water optical attenuation.

Another research investigates the association between acoustic emission cumulative energy and decreased cycling reversal loads in submerged concrete columns [23]. Ultrasonic surface waves are used to detect cracks in underwater concrete beams, with a Root Mean Square Deviation damage index used to analyze the wave data [24]. A method for assessing the concrete dams' blast resistance by investigating the induced vibration and crack penetration depth and use of a crack control agent to prevent failure of concrete structures is presented in [25,26].

2.3. Electrical methods: use of electrical resistance or capacitance to detect cracks, etc.

The coordination and electrostatic effects of water's optical absorption were resolved through computational analysis in [13]. A Monte Carlo calculation procedure was used in a computer simulation study to investigate the impact of photon incidence angle on the relationship between natural waters' visible and inherent optical characteristics in [27]. An approach that centers on water's inherent optical properties to fix water angular effects leaving brilliance was presented in [28].

2.4. Magnetic methods: use of magnetic fields to detect cracks, including the magnetic flux leakage method

Ground-penetrating radar, or GP radar, is a high-resolution, non-destructive technology for detecting hidden things via a high-frequency electromagnetic pulse. It has been widely used in a variety of fields including engineering/geologic research, underground historical research, to identify scour holes around bridge piers, and so on. It has also been used to assess the structural condition of underwater hydraulic structures [29].

2.5. Deep learning-based methods: image analysis of crack using deep learning.

Recently, neural networks have been increasingly applied to the quality of surface water estimation utilizing combined optical and microwave data. These networks excel in approximating nonlinear transfer functions, and as such, the research involved extracting data from water sample locations and analyzing digital data through various transformations [30]. In [31], A application for Windows was created to simulate and evaluate optical observations in aquatic settings..

Surface water detection is important for understanding flood hazards and potential damage to infrastructure and ecosystems. In [32,33] the applications of satellite remote sensing, and its limitation, in detecting and monitoring surface water, mapping, and parameter estimation are discussed.

An unsupervised method for identifying fractures in underwater concrete structures is offered in [34]. For eliminating outliers, the approach depends on local feature clustering utilizing K-Medians on Haralick texture characteristics with a dual Gaussian distribution. Detecting and classifying cracks in underwater dam structures based on sonar images is a difficult task due to the complexity of underwater environments and the random and diverse nature of cracks, as well as the low resolution of sonar images. In [35], a clustering analysis was performed on a 3D feature space to obtain crack fragments, which were then connected using an improved tensor voting method. [36] presents an alternate technique for identifying underwater dam breaches in sonar imagery. The cracked block tree (BT) approach comprises pre-processing low-resolution sonar pictures, breaking them down into

pieces for grouping analysis, and combining the crack segments with dynamic fragments of fracture based on tensor voting. In [37], a two-phase system is proposed for robust crack detection in concrete and pipelines inspections using Remotely Operated Vehicles. The [38] proposes a two-step approach for automatically identifying concrete fractures in aquatic situations. In the first step, the images are pre-processed through illumination balancing and image smoothing, and in the second step, a convolutional neural network (CNN) is used for crack detection.

In [39], a novel algorithm is proposed that generates a 3D spatial surface from the intensity values of a 2D image. The cracks are identified as "ditches" in the 3D surface, and their characteristics are analyzed using space curvatures. A BP neural network is then used to identify the crack objects. In [40], an artificial colony of bees algorithm-based edge extraction methodology is proposed. To improve the weak-object border gray contrast, an adaptive enhancement approach is applied, and a method of optimization using border direction information is presented to improve the edge extraction efficacy. [41] presents the establishment of a free aquatic light and turbid images repository (ULTIR) to assess the efficacy of image-based approaches for underwater structural evaluation.

In [42], an automatic crack detection method using image processing is proposed. The approach creates an augmented picture based on turbidity meter absorbance and eliminates the background component. Crack detection is performed using a decision tree learning algorithm. [43] presents a unique automated dam fracture detection technique that utilizes local-global clustering analysis. Using photographs, the system can precisely and rapidly detect faults on dam surfaces, decreasing human subjectivity.

In [44], it is conceived, prototyped, and tested a Tactile Imaging System for Underwater Inspection (TISUE). The device combines an elastomer-enabled contact-based optic sensor with specially designed artificial illumination to provide high-resolution and high-quality pictures of the structural damage to the surface in a turbid water environment. Finally, the paper [45] introduces the UIS-1 underwater inspection system, which comprises of a proprietary underwater robot and a unique quantitative analysis approach. The technology is tested in the field at the dam in Sichuan, China, and its efficacy is compared to that of other approaches. The suggested picture technique detects the coarse aggregate exposed automatically using SLIC super pixels and SVM machine learning, and the total exposure ratio is derived to assess the degree of abrasion.

2.6. Other methods: including the use of fiber optic sensors, thermal imaging, and X-ray imaging

Rendering water is a key component in creating natural scenes. In [46,47], we offer a method for creating accurate underwater optical effects using graphics hardware utilizing a Z-buffer, a stencil buffer, and an accumulation buffer. Additionally, [48] provides a strategy for evaluating the statistical distribution of water's level slopes using flash photography. Researchers introduced a temperature tracer approach for fracture identification in sub sea concrete structures based on heat transport theory in [49–51]. A method for controlling concrete cracking in underwater marine structures using basalt fiber is presented in [6].

The study presented in [52] developed a structural health monitoring tool that considered the reciprocal relationships and priority weights of different structural distresses to assess underwater structures. Cracking and collapse behaviors of an undersea shield tunnel's segmental liner construction exposed to a wrecked high-speed train collision were explored in [53]. In [54], researchers looked on the chaotic actions of arched concrete barriers subjected to underwater explosions. In addition, a system using a single camera deployed in a vehicle or robot was proposed in [55] to process a sequence of images and estimate crack dimensions.

Due to uneven lighting and considerable noise issues, detecting and classifying underwater dam breaches is difficult, and only a few approaches are adequate for this purpose. The study [56] presented a dodging algorithm to eliminate uneven illumination, based on an investigation of the statistical aspects of dam crack pictures, employing the regional features of block images and the global features of related domains. In [57], a simpler

approach for estimating the wear life of fractured concrete below water was developed, utilizing a changed design code that takes into account the crack's reduction in stress amplitude. [58] studies crack identification and categorization strategies based on crack kinds, and then implements Otsu's base thresholds method for crack detection, which is then utilized to construct the suggested crack detection system.

3. Challenges associated with underwater concrete crack detection

Working in underwater environments presents unique challenges that require specialized equipment and procedures for inspections. Underwater inspections require specialized diving equipment, including wet suits, diving masks, and tanks for air supply. Divers must be trained in specialized diving techniques, including decompression procedures and safety protocols. Additionally, specialized inspection equipment is necessary, such as underwater cameras, sonar devices, and non-destructive testing equipment.

One of the most significant difficulties in inspecting underwater concrete structures is detecting cracks. Underwater conditions, such as poor visibility, water pressure, and limited access, make it challenging to detect cracks. Visual inspections by divers are often necessary, but they can be time-consuming, expensive, and potentially hazardous. Advanced techniques such as ultrasonic testing, acoustic emission monitoring, and digital radiography are also used to detect cracks in underwater concrete structures.

Optical effects can also impact the quality of underwater images captured by unmanned aerial vehicles (UAVs) used for inspections. Optical effects such as refraction, reflection, and attenuation can distort images and impact the accuracy of inspections. To mitigate the impact of these optical effects, UAVs used for underwater inspections must be equipped with specialized cameras and sensors and operated by trained professionals who can account for these optical effects during inspections. Overall, working in underwater environments requires specialized equipment, procedures, and skills to overcome the unique challenges presented by the underwater environment.

4. Navigating challenges related to underwater concrete cracks detection using machine learning

Underwater concrete structures are critical components of many marine-based infrastructures, such as bridges, piers, and offshore oil platforms. Over time, these structures can develop cracks due to various factors, such as corrosion, water pressure, and natural wear and tear. Detecting and monitoring these cracks is essential for ensuring the safety and longevity of the structure. Visual inspection and dye penetrant testing are the traditional methods for crack detection, but they are time-consuming, expensive, and not always accurate. It has already been demonstrated by the works presented in [1,59] that machine learning approaches offer a much promising solution for detecting cracks in underwater concrete structures.

One approach to crack detection using machine learning is image processing of underwater concrete surfaces. Images of the concrete surface can be captured by underwater cameras and analyzed using machine learning algorithms to detect the presence of cracks. The first step in this approach is to capture high-quality images of the concrete surface. The images must be clear, well-lit, and taken at a close distance to the concrete surface. Once the images are captured, they are processed using image processing techniques such as edge detection, thresholding, and morphological operations. These techniques allow the machine learning algorithm to identify cracks in the images accurately.

Next, the images are fed into the machine learning algorithm for training. The algorithm is trained using a dataset of images with and without cracks. The algorithm learns to recognize the patterns in the images that indicate the presence of cracks. The dataset can be augmented to improve the algorithm's accuracy and generalizability.

Once the algorithm is trained, it can be used to detect cracks in new images of underwater concrete surfaces. The algorithm can be deployed on a computer or embedded in a camera system to perform real-time crack detection.

In conclusion, machine learning approaches based on image processing are a promising solution for crack detection in underwater concrete structures. With their high accuracy and efficiency, they offer a reliable way to detect and monitor cracks in these critical infrastructures.

In the next sections we will demonstrate the application of deep learning networks for identification of surface cracks in underwater structures. For this purpose we have used AlexNet and SqueezeNet through transfer learning approach on a large data-set of augmented images. The data set is generated such that it capture challenges associated with underwater effects.

5. The augmentation of the concrete cracks dataset

The impact of light on propagation events varies based on the seabed topography and streamer depth. By inputting these variables into an underwater wave propagation model, we can anticipate the locations where optical effects will affect the underwater visuals. Wave models are increasingly employed to study and forecast surf conditions in different coastal areas. These models can be developed using wave action or motion systems, which are also known as phase averaging or phase resolving models. The latest generation of phase average models is commonly used in various applications, including commercial tools for flow simulation and wave modeling in advanced professional engineering [59].

Oceanographers prioritize wave energy over wave amplitude. To analyze wave energy, they utilize a unique spectrum called $S(\omega)$, also referred to as a wave spectrum or frequency energy spectrum. This spectrum provides valuable insights into the distribution of wave energy based on frequency [60]. Pierson and Moskowitz [61] developed a formula for the ocean that incorporates wind speed as a factor. However, in a fetch-limited sea with increasing waves, the JONSWAP spectrum has been demonstrated to be more suitable and effective (Hasselmann et al.).[62]:

$$S_J(\omega) = \frac{\alpha g^2}{\omega^5} \exp\left(-\frac{5}{4}\left(\frac{\omega_p}{\omega}\right)^4\right) \gamma \exp\left(-\frac{(\omega-\omega_p)^2}{2\sigma^2\omega_p^2}\right) \quad (1)$$

The symbol ω_p represents the frequency at which the spectrum reaches its peak. The typical value for ω_p is $\omega_p = 0.855$, with U_{10} denoting the wind speed at a height of 10 meters above the sea surface. In this context, γ represents the peak enhancement factor, and parameter σ indicates the width of the peak. The specific values for these parameters in the spectrum equation are:

$$\alpha = 0.076 \left(\frac{U_{10}^2}{Fg}\right)^{0.22}, \omega_p = 22 \left(\frac{g^2}{U_{10}F}\right)^{1/3}, \sigma = \begin{cases} 0.07, \omega \leq \omega_p \\ 0.09, \omega > \omega_p \end{cases}$$

where F is the fetch in meters, usually $\gamma = 3.3$, but can vary from 1 to 7.

The JONSWAP spectrum is used in this study since the fetch is vital for the description of the sea state.

The equation $S(\omega, \theta) = S_J(\omega)G(\omega, \theta)$ denotes spectrum of sea waves and is used for the description of characteristics of the wave direction, the $G(\omega, \theta)$ follows:

$$G(\omega, \theta) = \frac{1}{\pi} \left\{ 1 + \left[0.5 + 0.82 \exp\left(-\frac{\left(\frac{\omega}{\omega_p}\right)^4}{2}\right) \right] \cos 2\theta + 0.32 \exp\left(-\frac{\left(\frac{\omega}{\omega_p}\right)^4}{2}\right) \cos 4\theta \right\} \quad (2)$$

The extension feature suggested by the stereo wave observation project (SWOP) [63] is employed in this study. The elevation of the sea surface $H(x, y, t)$ is expressed by the Double Summation Model [64]:

$$H(x, y, t) = \sum_{i=1}^{\infty} \sum_{j=1}^{\infty} \sqrt{2S(\omega_i, \theta_i)\Delta\omega_i\Delta\theta_i} \cos(k_i x \cos \theta_j + k_i y \sin \theta_j - \omega_i t - \varepsilon_{ij}) \quad (3)$$

where a_{ij} is the wave amplitude of frequency i and directional angle j , the directional angle of the wave θ_j ($0 < \theta \leq 2\pi$), the frequency is ω_i , the wave number k_i is equal to $k_i = \omega_i^2/2$, the random initial phase angle ε_{ij} ($0 \leq \varepsilon_{ij} < 2\pi$).

The 3D waves of the ocean are simulated using MATLAB, a mathematical tool with a broad range of graphic processing capabilities. By examining the ideal illustration of the JONSWAP spectrum and SWOP directed expansion function under $U = 20m/s$, the right range of frequency as well as the angles for equalization is developed, and an interactive seafloor wave models at certain times over an established sea area is created. The frequency equal division method was utilized to numerically reproduce the average frequency using an angular frequency in the $[0.01, 4]$ range. Parameters N and M equal to 35, $\Delta\omega = 0.114rad/s$, $\Delta\theta = 0.0898rad$, the directional angle is $[-\pi/2, \pi/2]$. The computation results over 1 - 2 seconds are illustrated in Fig. 1:

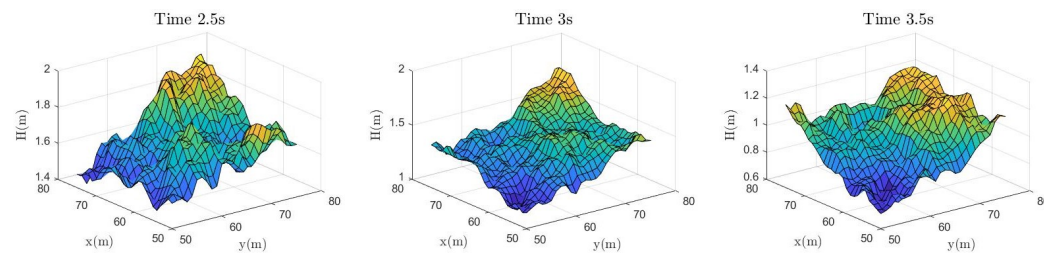


Figure 1. Figure showing water surface deformations at different times

The representation of water surface interconnection with light is highly important and achievable via reflections, refractions, and light absorption. The determination of the quantity of light coming to the point of view can be computed as presented in [65]. The behavior of lights traveling through the water surface is illustrated in the Fig 2.

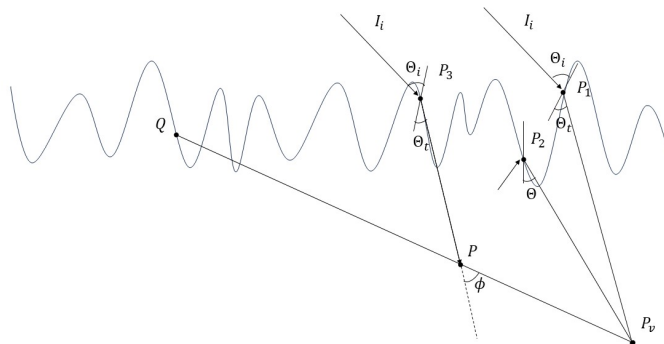


Figure 2. Aspects of reflection of lights due to the surface undulations. The component of refracted light in the incident light at a point on the water surface enters the vantage point at P_1 and P_3 . The light that is perfectly reflected at a point on the water surface enters the vantage point at P_2 . The light is scattered and attenuated by particles along the way at P . The viewpoint is remarked as P_v , the reflected light is noted at point Q .

The quantity of light $I_v(\lambda)$ traveling from the point on the water surface Q to perspective I_v while observation is from the underwater can be computed by [65]:

$$I_v(\lambda) = I_Q(\lambda) \exp(-c(\lambda)L) + \int_0^L I_P(\lambda) \exp(-c(\lambda)l) dl \quad (4)$$

where L represents the distance between P_vQ , l - the distance between PP_v , $c(\lambda)$ depicts the attenuation coefficient of the light, the intensity of light at point P is represented by I_P (Fig. 2).

The technique for rendering optical effects with graphic equipment are presented in [66] and related to the generation of illumination volumes (Fig. 3). 306
307

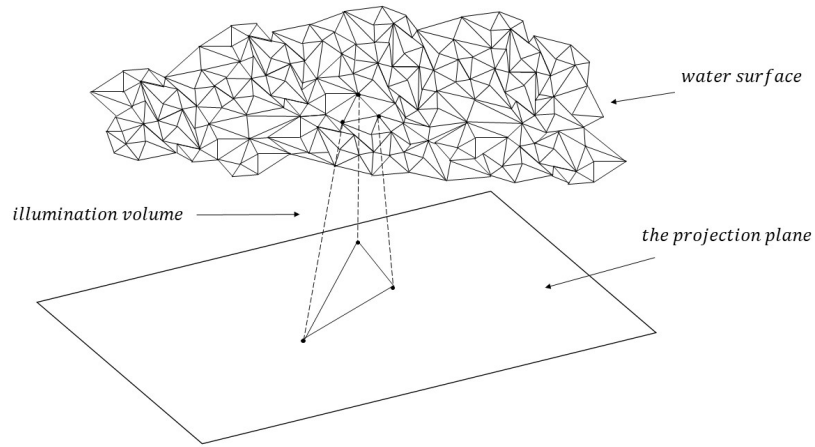


Figure 3. The generation of illumination volumes. 311
312
313
314
315
316
317
318
319
320
321
322
323
324

In this study it is important to have realistic images of underwater concrete structures, so technique for rendering illumination effects is presented in [59]. First, it is assumed that the surface of the water is level, and the sun's refraction vector is detected. Then, the texture of the surface is developed, representing depth of the underwater. Finally, the perspective of the scene is chosen as of the human eye. This method was developed with the Blender program [59].

The test of the deep learning methods was performed using concrete crack images with and without underwater optical effects. The method used for the generation of underwater optical effects is presented in [59]. The collection contains 40000 photos of surface with and without concrete fractures (20000 with cracks - "Positive", and 20000 without cracks - "Negative") from Ozgecracksnel's released data set is used for the test [67]. Optical water illusion effects were generated using the technique depicted in [59] and various modifications (random rotation, zoom, height, width) and different blending techniques were employed for the the dataset augmentation. For the image classification 40000 distinct optical underwater effects were generated and applied for the whole dataset of images with and without cracks 4. The technique of the image augmentation is presented detailed in [59].

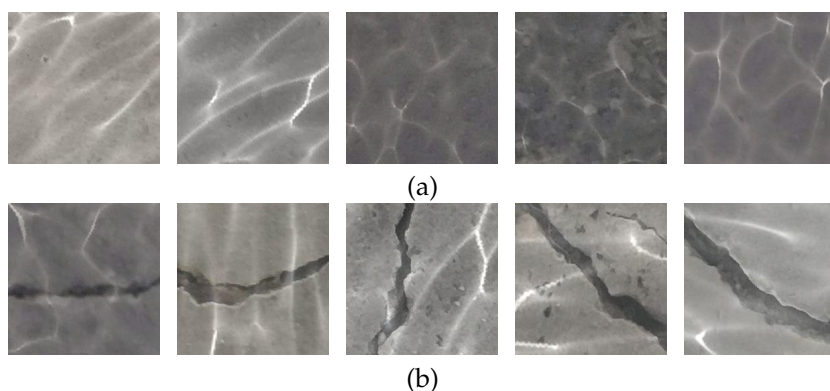


Figure 4. Example of augmented dataset. Concrete images without cracks and with underwater optical effects are depicted in panel (a). Concrete images with cracks and with underwater optical effects are depicted in panel (b). 325
326

Machine learning methods used for the image classification are presented in the next section.

6. Underwater concrete crack detection using machine learning approaches

Cracks in underwater concrete structures can significantly impact their structural integrity and longevity. As described in sections above the traditional methods for detecting cracks in underwater structures are often time-consuming, costly, and require skilled operators. In recent years, machine learning approaches have shown promise for detecting cracks in underwater structures quickly and accurately in onshore environmental conditions [1,2]. In this section we explore the potential of using machine learning based approaches to identify surface cracks on concrete structures in underwater conditions. The concrete cracks in underwater environment are impacted by illumination and presence of marine life, which makes the problem harder to solve compared to surface crack detection in onshore or above water environment. Two tests are conducted: First, test involve using standard machine learning network Alexnet [2] trained on surface crack detection for onshore environment described in [1] is used to identify underwater cracks. Next, test involves an improved version of the network presented in [1], where the network is further trained using augmented underwater images database prepared in [59]. The two test cases and their results are presented next.

6.1. Transfer Learning and use of pre-trained network

The machine learning approach employed in this paper utilizes transfer learning for training, testing, and validation purposes. This approach is chosen for several reasons. Firstly, it enables the evaluation of various well-established deep learning networks. Moreover, transfer learning saves time by eliminating the need to develop a network from scratch, which can be a challenging task requiring expertise in network design. Furthermore, implementing the transfer learning approach is straightforward and facilitates faster simulation, leading to improved sensitivity within a relatively short time-frame for real-world applications.

The underlying concept of transfer learning involves leveraging a pre-trained network's knowledge and applying it to a similar task by training or exposing it to an additional set of parameters. In the context of this paper, which focuses on image classification, there are several existing pre-trained image classification networks such as SqueezeNet and AlexNet. These networks have been trained to classify a wide range of images, surpassing 1000 categories. Therefore, it is possible to select one of these networks and retrain it for a new classification task. This retraining process involves adjusting some network parameters to classify a fresh set of images. Fine-tuning the parameters of a pre-trained network is considerably faster and easier compared to building a network from scratch. The paper follows this precise approach, and for more detailed information on creating transfer learning networks, please refer to [68].

6.2. Test cases - Review of performance of existing networks on concrete image with and without crack and underwater effects

Detecting cracks on underwater surfaces poses a significant challenge, and conventional image detection networks cannot be directly applied to this problem. To demonstrate the limitations of currently available networks, we conducted a series of tests using a concrete crack dataset, as outlined in our published papers [1,2]. The methodology is based on transfer learning, which is described in detail in [68]. Our evaluation comprised two tests: the first involved training a network to distinguish between crack and non-crack surfaces, while the second tested the same network's ability to detect cracks under conditions of underwater illumination (see Figure 5 and Figure 6 for sample images used in both tests). To conduct our study, we employed two distinct image datasets:

1. Concrete crack images dataset. Example of this dataset is shown in Figure 5.

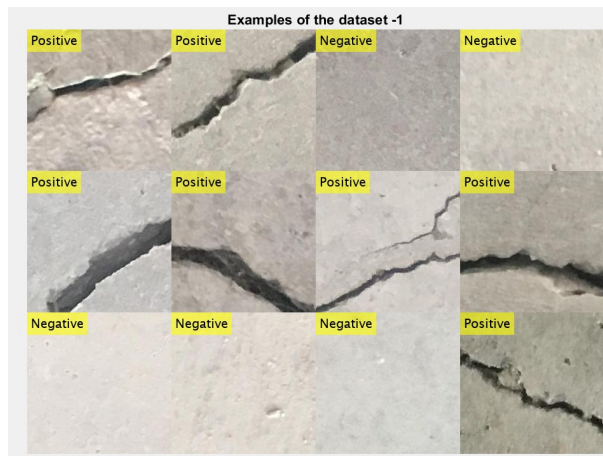


Figure 5. Concrete crack images dataset example

2. Underwater crack images dataset. Example of this dataset is shown in Figure 6.

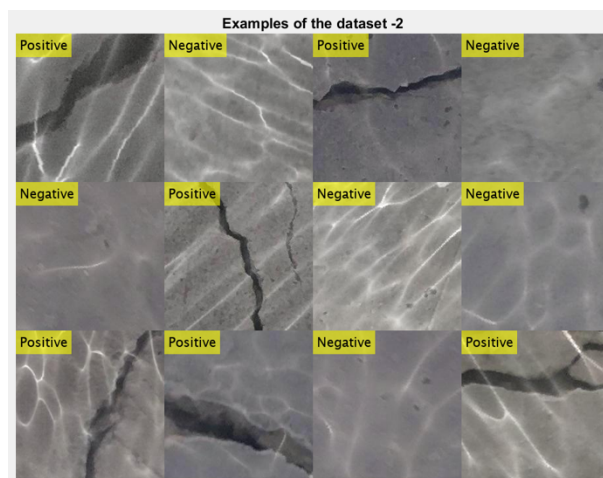


Figure 6. Underwater crack images dataset example

6.3. *Test Case 1: Testing trained network on identify crack with non-crack surfaces and using same network to test underwater images*

In this case we used a trained network [1] for identification of crack with non-crack surfaces in various outdoor setting. The Case 1 characteristics and techniques:

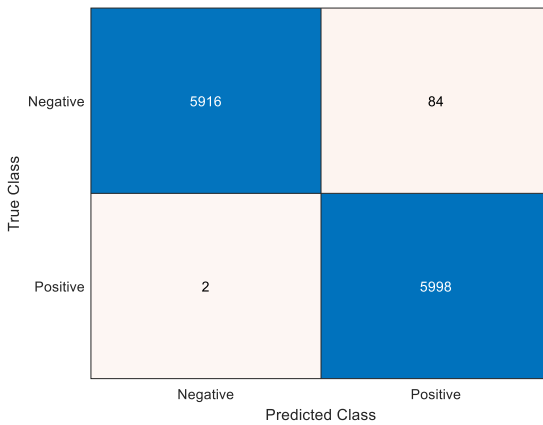
- Training was conducted on concrete crack images dataset;
- Testing was conducted on underwater crack images dataset;
- For case investigation we used convolutional neuron network (CNN) architecture AlexNet and SqueezeNet.

For Case 1 investigation we used different training data, testing data and validation data parameters that are shown along with the accuracy of the network in Table 1. It can be seen from the results that network accuracy in most cases is above 99 %. Two different networks trained using transfer learning approaches described in [1] are used, namely Alexnet and SqueezeNet. Based on Table 1 we can see that using AlexNet architecture we get the best results when we use these parameters: TrainingData=0.3; TestingData=0.3; ValidationData =0.3.

The results of this case are presented in Figure 7 and Figure 8. It can be seen from these results that when the network is trained on identifying cracks in surfaces which are in outdoor setting it works well, above 99 % accuracy, but the performance of same network in identifying cracks in underwater images is rather poor, close to 92 % accuracy only.

Table 1. SqueezeNet and AlexNet architecture results

Index	Parameters used for Training Network	Overall Accuracy for concrete crack dataset	Overall Accuracy for under-water crack dataset	Validation accuracy	Training time	Epoch	Maximum Iterations	Iterations per epoch	Frequency	Learning rate
SqueezeNet										
1.	Training - 0.1, Testing - 0.1, Validation - 0.1	99.2 %	84 %	97.78 %	54 min 29 sec	6	186	31	30 iterations	0.001
2.	Training - 0.15, Testing - 0.15, Validation - 0.1	98 %	70 %	97.80 %	87 min 23 sec	6	276	46	30 iterations	0.001
3.	Training - 0.3, Testing - 0.3, Validation - 0.3	99.3 %	61 %	99.17 %	104 min 13 sec	6	558	93	30 iterations	0.001
AlexNet										
1.	Training - 0.1, Testing - 0.1, Validation - 0.1	99.5 %	79 %	99.75 %	39 min 47 sec	6	186	31	30 iterations	0.001
2.	Training - 0.15, Testing - 0.15, Validation - 0.1	99.7 %	87 %	99.72 %	56 min 19 sec	6	276	46	30 iterations	0.001
3.	Training - 0.3, Testing - 0.3, Validation - 0.3	99.7 %	92 %	99.83 %	115 min 32 sec	6	558	93	30 iterations	0.001

**Figure 7.** Confusion matrix with concrete crack images dataset (Overall Accuracy=99.7 %)

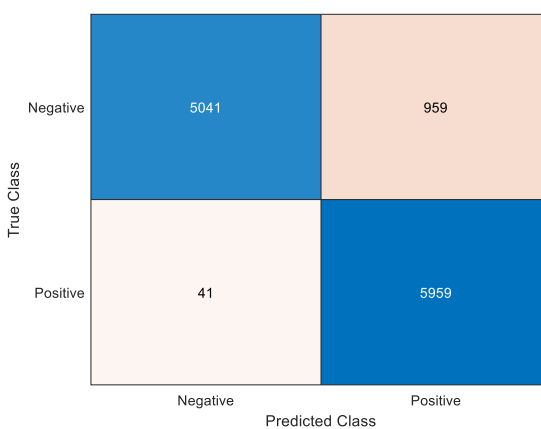


Figure 8. Confusion matrix with underwater crack images dataset (Overall Accuracy=92 %)

6.4. Test Case 2: Testing trained network to identify crack with non-crack surfaces on identifying cracks in underwater images

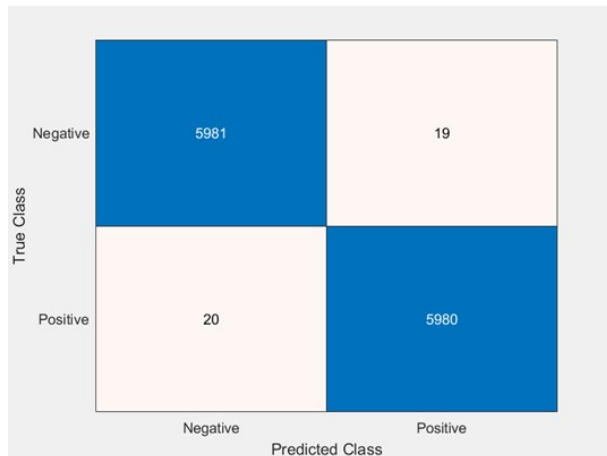
In this case we used a trained network used in case 1 with additional images, which are augmented to take into account underwater effects, e.g., illumination, shades, colour etc. The trained network is then used for identification of crack with non-crack surfaces in various outdoor setting as well as to identify crack on underwater images with illumination effects. The Case 2 characteristics and techniques:

- Training was conducted on underwater crack images dataset;
- Testing was conducted on underwater crack images dataset;
- For case investigation we used convolutional neural network (CNN) architecture AlexNet and SqueezeNet.

For Case 2 investigation we used different training data, testing data and validation data parameters that are shown in a final Case 2 investigation results table (Table 2). Based on Table 2 we can see that using AlexNet architecture we get the best results when we use these parameters: TrainingData=0.3; TestingData=0.3; ValidationData =0.3. The results of this case are presented in Figure 9. The results of this case show that with additional argument images of underwater effects, the network accuracy is improved to above 99 %.

Table 2. SqueezeNet and AlexNet architecture results

Index	Parameters used for Training Network	Overall Accuracy for under-water crack dataset	Validation accuracy	Training time	Epoch	Maximum Iterations	Iterations per epoch	Frequency	Learning rate
SqueezeNet									
1.	Training - 0.1, Testing - 0.1, Validation - 0.1	98.25 %	99.12 %	74 min 54 sec	6	186	31	30 iterations	0.001
2.	Training - 0.15, Testing - 0.15, Validation - 0.1	99.1 %	99.20 %	124 min 27 sec	6	276	46	30 iterations	0.001
3.	Training - 0.3, Testing - 0.3, Validation - 0.3	99.6 %	99.45 %	282 min 49 sec	6	558	93	30 iterations	0.001
AlexNet									
1.	Training - 0.1, Testing - 0.1, Validation - 0.1	99.6 %	99.62 %	460 min 20 sec	6	186	31	30 iterations	0.001
2.	Training - 0.15, Testing - 0.15, Validation - 0.1	99.5 %	99.47 %	450 min 51 sec	6	276	46	30 iterations	0.001
3.	Training - 0.3, Testing - 0.3, Validation - 0.3	99.7 %	99.67 %	355 min 27 sec	6	558	93	30 iterations	0.001

**Figure 9.** Confusion matrix with underwater crack images dataset (Overall Accuracy=99.7 %)

The two test cases presented here demonstrates that its possible to improve the performance of existing networks by training them using augmented images such that the network will become capable of identifying surface cracks in onshore as well as offshore under water conditions too. Network accuracy could be further improved through parameter optimization and even better/rich database of augmented images.

7. Conclusion

The paper focuses on the development of an underwater crack detection system for structural integrity assessment of submerged structures, emphasizing the use of machine learning approaches. This highlights the significance of advanced technology in addressing the challenges associated with underwater crack detection.

The literature review conducted in the paper provides insights into the current methods for underwater surface crack detection, highlighting the existing challenges and potential opportunities for improvement. This suggests that the proposed system takes into account the limitations of current approaches and aims to overcome them.

The paper introduces an image augmentation approach for creating underwater optical effects. By utilizing augmented images, the proposed system enhances the performance of existing network-based machine learning approaches in detecting cracks in underwater conditions. This showcases the innovative use of data augmentation techniques to improve detection accuracy.

The experimental results presented in the paper demonstrate the effectiveness and accuracy of the developed system in detecting cracks in underwater structures. This indicates that the proposed system has the potential to significantly contribute to the safety and reliability of submerged structures, such as offshore oil and gas installations, underwater pipelines, and underwater foundations for bridges and dams.

The implementation of the proposed system has the potential to prevent catastrophic failures by detecting cracks in underwater structures at an early stage. This emphasizes the importance of proactive maintenance and inspection strategies, which can ultimately save costs and ensure the long-term integrity of underwater infrastructure.

References

1. Palevičius, P.; Pal, M.; Landauskas, M.; Orinaitė, U.; Timofejeva, I.; Ragulskis, M. Automatic Detection of Cracks on Concrete Surfaces in the Presence of Shadows. *Sensors* **2022**, *22*. <https://doi.org/10.3390/s22103662>.
2. Pal, M.; Palevičius, P.; Landauskas, M.; Orinaitė, U.; Timofejeva, I.; Ragulskis, M. An Overview of Challenges Associated with Automatic Detection of Concrete Cracks in the Presence of Shadows. *Applied Sciences* **2021**, *11*. <https://doi.org/10.3390/app112311396>.
3. Cox, C.; Munk, W. Some problems in optical oceanography. *Journal of marine research* **1955**, *1*, 63–78.
4. Zhong, N.; Zhu, X.; Q.Liao.; Y.Wang.; Chen, R.; Sun, Y. Effects of surface roughness on optical properties and sensitivity of fiber-optic evanescent wave sensors. *Applied optics* **2013**, *52*, 3937–45. <https://doi.org/10.1364/AO.52.003937>.
5. Li, H.; Han, C. Sonochemical Synthesis of Cyclodextrin-Coated Quantum Dots for Optical Detection of Pollutant Phenols in Water. *Chemistry of Materials - CHEM MATER* **2008**, *20*. <https://doi.org/10.1021/cm8009176>.
6. Legleiter, C.; Roberts, D.; W.Marcus.; Fonstad, M. Passive optical remote sensing of river channel morphology and in-stream habitat: Physical basis and feasibility. *Remote Sensing of Environment* **2004**, *93*, 493–510. <https://doi.org/10.1016/j.rse.2004.07.019>.
7. Gordon, H.R.; Ding, K. Self-shading of in-water optical instruments. *Limnology and Oceanography* **1992**, *37*, 491–500, [<https://aslopubs.onlinelibrary.wiley.com/doi/pdf/10.4319/lo.1992.37.3.0491>]. <https://doi.org/https://doi.org/10.4319/lo.1992.37.3.0491>.
8. Dong, Y.; Tang, S.; Zhang, X. Effect of Random Sea Surface on Downlink Underwater Wireless Optical Communications. *IEEE Communications Letters* **2013**, *17*, 2164 – 2167. <https://doi.org/10.1109/LCOMM.2013.091113.131363>.
9. Yoshimori, K.; Itoh, K.; Ichioka, Y. Optical characteristics of a wind-roughened water surface: a two-dimensional theory. *Appl. Opt.* **1995**, *34*, 6236–6247. <https://doi.org/10.1364/AO.34.006236>.
10. Huang, C.; Chen, Y.; Zhang, S.; Wu, J. Detecting, Extracting, and Monitoring Surface Water From Space Using Optical Sensors: A Review. *Reviews of Geophysics* **2018**, *56*. <https://doi.org/10.1029/2018RG000598>.
11. Shi, H.; Itoh, M.; Takami, T. Optical Observation of the Supercavitation Induced by High-Speed Water Entry. *Journal of Fluids Engineering* **2000**, *122*, 806–810, [https://asmedigitalcollection.asme.org/fluidsengineering/article-pdf/122/4/806/5615001/806_1.pdf]. <https://doi.org/10.1115/1.1310575>.
12. Smart, J. Underwater optical communications systems part 1: variability of water optical parameters. In Proceedings of the MILCOM 2005 - 2005 IEEE Military Communications Conference, 2005, pp. 1140–1146 Vol. 2. <https://doi.org/10.1109/MILCOM.2005.1605832>.
13. Hermann, A.; Schmidt, W.G.; Schwerdtfeger, P. Resolving the Optical Spectrum of Water: Coordination and Electrostatic Effects. *Phys. Rev. Lett.* **2008**, *100*, 207403. <https://doi.org/10.1103/PhysRevLett.100.207403>.
14. Steele, H.M.; Hamill, P. Effects of temperature and humidity on the growth and optical properties of sulphuric acid—water droplets in the stratosphere. *Journal of Aerosol Science* **1981**, *12*, 517–528. [https://doi.org/https://doi.org/10.1016/0021-8502\(81\)90054-9](https://doi.org/https://doi.org/10.1016/0021-8502(81)90054-9).
15. Jou, F.Y.; Freeman, G.R. Temperature and isotope effects on the shape of the optical absorption spectrum of solvated electrons in water. *The Journal of Physical Chemistry* **1979**, *83*, 2383–2387.
16. Witte, W.G.; Whitlock, C.H.; C.Harriss, R.; Usry, J.W.; Poole, L.R.; Houghton, W.M.; Morris, W.D.; Gurganus, E.A. Influence of dissolved organic materials on turbid water optical properties and remote-sensing reflectance. *Journal of Geophysical Research: Oceans* **1982**, *87*, 441–446, [<https://agupubs.onlinelibrary.wiley.com/doi/pdf/10.1029/JC087iC01p00441>]. <https://doi.org/https://doi.org/10.1029/JC087iC01p00441>.
17. Momen, M.; D.Wood, J.; Novick, K.A.; Pangle, R.; Pockman, W.T.; McDowell, N.G.; Konings, A.G. Interacting Effects of Leaf Water Potential and Biomass on Vegetation Optical Depth. *Journal of Geophysical Research: Biogeosciences* **2017**, *122*, 3031–3046, [<https://agupubs.onlinelibrary.wiley.com/doi/pdf/10.1002/2017JG004145>]. <https://doi.org/https://doi.org/10.1002/2017JG004145>.

18. Thornton, B. Effects of Pressure on the Optical Emissions Observed from Solids Immersed in Water Using a Single Pulse Laser. *Applied Physics Express* **2011**, *4*, 2702–. <https://doi.org/10.1143/APEX.4.022702>. 483
484

19. Hill, R.J. Optical propagation in turbulent water. *J. Opt. Soc. Am.* **1978**, *68*, 1067–1072. <https://doi.org/10.1364/JOSA.68.001067>. 485

20. Stavn, R.H.; Weidemann, A.D. Optical modeling of clear ocean light fields: Raman scattering effects. *Appl. Opt.* **1988**, *27*, 4002–4011. <https://doi.org/10.1364/AO.27.004002>. 486
487

21. Gilvear, D.; Hunter, P.; Higgins, T. An experimental approach to the measurement of the effects of water depth and substrate on optical and near infra-red reflectance: a field-based assessment of the feasibility of mapping submerged instream habitat. *International Journal of Remote Sensing* **2007**, *10*, 2241–2256. <https://doi.org/10.1080/01431160600976079>. 488
489

22. Bristow, M.; Nielsen, D.; Bundy, D.; Furtek, R. Use of water Raman emission to correct airborne laser fluorosensor data for effects of water optical attenuation. *Appl. Opt.* **1981**, *20*, 2889–2906. <https://doi.org/10.1364/AO.20.002889>. 490
491

23. Jiang, A.L.; Zhao, Y.H.; Zhang, L.W. Experimental study of acoustic emission characteristics of underwater concrete structures. *2008 Symposium on Piezoelectricity, Acoustic Waves, and Device Applications* **2008**, pp. 252–257. 492
493

24. Baharom, S.; Mutlib, N.K.; El-Shafie, A. Crack detection of Underwater Concrete Beams Using Ultrasonic Surface Waves. *The 2015 World Congress on Advances in Structural Engineering and Mechanics (ASEM15)* **2015**. 494
495

25. Wang, C.; Wei, P.; H.Wang, X.; Zhang, S.; Cui, W. Blast-Resistance and Damage Evaluation of Concrete Gravity Dam Exposed to Underwater Explosion: Considering the Initial Stress Field. *KSCE Journal of Civil Engineering* **2021**, *25*. <https://doi.org/10.1007/s12205-021-1650-0>. 496
497

26. Hamid, H.; Chorzepa, M.G.; Durham, S.A. Investigation of Cracks Observed in Underwater Bridge Seal Structures and Crack Control by Means of Material Design. *Journal of Performance of Constructed Facilities* **2020**, *34*, 04020117. [https://doi.org/10.1061/\(ASCE\)CF.1943-5509.0001523](https://doi.org/10.1061/(ASCE)CF.1943-5509.0001523). 498
499

27. Kirk, J.T.O. Dependence of relationship between inherent and apparent optical properties of water on solar altitude. *Limnology and Oceanography* **1984**, *29*, 350–356, [<https://aslopubs.onlinelibrary.wiley.com/doi/pdf/10.4319/lo.1984.29.2.0350>]. <https://doi.org/https://doi.org/10.4319/lo.1984.29.2.0350>. 500
501

28. Lee, Z.P.; Du, K.; Voss, K.J.; Zibordi, G.; Lubac, B.; Arnone, R.; Weidemann, A. An inherent-optical-property-centered approach to correct the angular effects in water-leaving radiance. *Appl. Opt.* **2011**, *50*, 3155–3167. <https://doi.org/10.1364/AO.50.003155>. 502
503

29. Xingxin, X.; Jin, W.; Jinyin, S.; Zaicheng, H. Case Study: Application of GPR to Detection of Hidden Dangers to Underwater Hydraulic Structures. *Journal of Hydraulic Engineering* **2006**, *132*, 12–20. [https://doi.org/10.1061/\(ASCE\)0733-9429\(2006\)132:1\(12\)](https://doi.org/10.1061/(ASCE)0733-9429(2006)132:1(12)). 504
505

30. Zhang, Y.; Pullainen, J.; S.Koponen.; Hallikainen, M. Application of an empirical neural network to surface water quality estimation in the Gulf of Finland using combined optical data and microwave data. *Remote Sensing of Environment* **2002**, *81*, 327–336. [https://doi.org/10.1016/S0034-4257\(02\)00009-3](https://doi.org/10.1016/S0034-4257(02)00009-3). 506
507

31. Gege, P. The water color simulator WASI: an integrating software tool for analysis and simulation of optical in situ spectra. *Computers Geosciences* **2004**, *30*, 523–532. <https://doi.org/https://doi.org/10.1016/j.cageo.2004.03.005>. 508
509

32. Musa, Z.N.; Popesc, I.; Mynett, A. A review of applications of satellite SAR, optical, altimetry and DEM data for surface water modelling, mapping and parameter estimation. *Hydrology and Earth System Sciences* **2015**, *19*, 3755–3769. <https://doi.org/10.5194/hess-19-3755-2015>. 510
511

33. Irwin, K.; D.Beaulne.; Braun, A.; Fotopoulos, G. Fusion of SAR, Optical Imagery and Airborne LiDAR for Surface Water Detection. *Remote Sens* **2017**, *890*. <https://doi.org/10.3390/rs9090890>. 512
513

34. Mucolli, L.; S.rupinski, K.; F.Maurelli.; Mehdi, S.A.; Mazhar, S. Detecting cracks in underwater concrete structures: an unsupervised learning approach based on local feature clustering. *10* 2019, pp. 1–8. <https://doi.org/10.23919/OCEANS40490.2019.8962401>. 514
515

35. Shi, P.; Fan, X.; J., N.; Khan, Z.; Li, M. A novel underwater dam crack detection and classification approach based on sonar images. *PLoS one* **2017**, *12*, e0179627. <https://doi.org/doi.org/10.1371/journal.pone.0179627>. 516
517

36. Shi, P.; Fan, X.; Wang, G. A novel underwater dam crack detection algorithm based on sonar images. *01* 2016. <https://doi.org/10.2991/iccsae-15.2016.85>. 518
519

37. El-Messiry, H.; Khaled, H.; Maher, A.; Ahmed, A. Real-Time Crack Detection Using ROV. *Lecture Notes in Networks and Systems - Intelligent Computing* **2021**, pp. 922–929. 520
521

38. Qi, Z.; Zhang, J.; Liu, D., A CNN-Based Method for Concrete Crack Detection in Underwater Environments. In *Construction Research Congress 2020*; pp. 566–575. <https://doi.org/10.1061/9780784482865.060>. 522
523

39. Chen, C.; Wang, J.; Zou, L.; Fu, J.; Ma, C.J. A novel crack detection algorithm of underwater dam image. *2012 International Conference on Systems and Informatics, ICSAI 2012* **2012**. <https://doi.org/10.1109/ICSAI.2012.6223399>. 524
525

40. Zhang, Z.; Fan, X.; Xie, Y.; Xu, H. An edge detection method based artificial bee colony for underwater dam crack image. *04* 2018, p. 59. <https://doi.org/10.1117/12.2316618>. 526
527

41. O'Byrne, M.; Schoefs, F.; Pakrashi, V.; Ghosh, B. An underwater lighting and turbidity image repository for analysing the performance of image-based non-destructive techniques. *Structure and Infrastructure Engineering* **2017**, *14*, 1–20. <https://doi.org/10.1080/15732479.2017.1330890>. 528
529

42. Yuya, N.; Naoto, S.; Shinsuke, Y.; Kazuo, I. Crack Detection in a Concrete Structure Using an Underwater Vehicle. *01* 2021, pp. 777–781. <https://doi.org/10.5954/ICAROB.2021.OS23-1>. 530
531

43. Fan, X.; Wu, J.; Shi, P.; Zhang, X.; Xie, Y. A novel automatic dam crack detection algorithm based on local-global clustering. *Multimedia Tools and Applications* **2018**, *77*. <https://doi.org/10.1007/s11042-018-5880-1>. 541
542

44. Chen, X.; Wu, G.; Hou, S.; Fan, J.; Dang, J.; Chen, Z. Development of Tactile Imaging for Underwater Structural Damage Detection. *Sensors* **2019**, *18*, 3925. <https://doi.org/10.3390/s19183925>. 543
544

45. Li, Y.; Zhang, H.; Wang, S.; Li, J. Image-Based Underwater Inspection System for Abrasion of Stilling Basin Slabs of Dam. *Advances in Civil Engineering* **2019**, *2019*, 1–13. <https://doi.org/10.1155/2019/6924976>. 545
546

46. Iwasaki, K.; Dobashi, Y.; Nishita, T. An Efficient Method for Rendering Underwater Optical Effects Using Graphics Hardware. *Computer Graphics Forum* **2002**, *21*, 701–711, [<https://onlinelibrary.wiley.com/doi/pdf/10.1111/1467-8659.00628>]. <https://doi.org/https://doi.org/10.1111/1467-8659.00628>. 547
548

47. Nishita, T.; Nakamae, E. Method of Displaying Optical Effects within Water Using Accumulation Buffer. In Proceedings of the Proceedings of the 21st Annual Conference on Computer Graphics and Interactive Techniques, New York, NY, USA, 1994; SIGGRAPH '94, p. 373–379. <https://doi.org/10.1145/192161.192261>. 550
551

48. Schooley, A.H. A Simple Optical Method for Measuring the Statistical Distribution of Water Surface Slopes. *J. Opt. Soc. Am.* **1954**, *44*, 37–40. <https://doi.org/10.1364/JOSA.44.000037>. 553
554

49. Chen, J.; Xiong, F.; Zhu, Y.; Yan, H. A crack detection method for underwater concrete structures using sensing-heating system with porous casing. *Measurement* **2021**, *168*, 108332. <https://doi.org/https://doi.org/10.1016/j.measurement.2020.108332>. 555
556

50. Zhu, Y.; J.Chen.; Y.Zhang.; Xiong, F.; He, F.; Fang, X. Temperature tracer method for crack detection in underwater concrete structures. *Structural Control and Health Monitoring* **2020**, *27*, e2595, [<https://onlinelibrary.wiley.com/doi/pdf/10.1002/stc.2595>]. e2595 STC-20-0002.R3, <https://doi.org/https://doi.org/10.1002/stc.2595>. 557
558

51. Zhang, C.; J.en, C.; Y.Luo.; Xiong, F. Crack width identification for underwater concrete structures using temperature tracer method. *Measurement Science and Technology* **2021**, *32*. <https://doi.org/10.1088/1361-6501/ac20b5>. 560
561

52. Yi, N.H.; Nam, J.W.; Kim, S.B.; Kim, I.S.; Kim, J.H.J. Evaluation of material and structural performances of developed Aqua-Advanced-FRP for retrofitting of underwater concrete structural members. *Construction and Building Materials* **2010**, *24*, 566–576. <https://doi.org/https://doi.org/10.1016/j.conbuildmat.2009.09.008>. 562
563

53. Yan, Q.; Xu, Y.; Zhang, W.; Geng, P.; Yang, W. Numerical analysis of the cracking and failure behaviors of segmental lining structure of an underwater shield tunnel subjected to a derailed high-speed train impact. *Tunnelling and Underground Space Technology* **2018**, *72*, 41–54. <https://doi.org/https://doi.org/10.1016/j.tust.2017.11.002>. 565
566

54. Moradloo, A.; Adib, A.; Pirooznia, A. Damage Analysis of Arch Concrete Dams Subjected to the Underwater Explosion. *Applied Mathematical Modelling* **2019**. <https://doi.org/10.1016/j.apm.2019.04.064>. 568
569

55. Lins, R.G.; Givigi, S.N. Automatic Crack Detection and Measurement Based on Image Analysis. *IEEE Transactions on Instrumentation and Measurement* **2016**, *65*, 583–590. 570
571

56. Shi, P.; Fan, X.; Ni, J.; Wang, G. A detection and classification approach for underwater dam cracks. *Structural Health Monitoring* **2016**, *15*, 541–554, [<https://doi.org/10.1177/1475921716651039>]. <https://doi.org/10.1177/1475921716651039>. 572
573

57. Miura, T.; Sato, K.; Nakamura, H. Influence of primary cracks on static and fatigue compressive behavior of concrete under water. *Construction and Building Materials* **2021**, *305*, 124755. <https://doi.org/https://doi.org/10.1016/j.conbuildmat.2021.124755>. 574
575

58. N., S.S.; Kavitha, S.; Raghuraman, G. Review and Analysis of Crack Detection and Classification Techniques based on Crack Types. *International Journal of Applied Engineering Research* **2021**. 576
577

59. Orinaitė, U.; Palevičius, P.; Pal, M.; Ragulskis, M. A deep learning-based approach for automatic detection of concrete cracks below the waterline. *Vibroengineering Procedia* **2022**, *44*. <https://doi.org/https://doi.org/10.21595/vp.2022.22845>. 578
579

60. Fréchot, J. Realistic simulation of ocean surface using wave spectra. *International Conference on Computer Graphics Theory and Applications* **2006**. 580
581

61. Pierson, W.J.; Moskowitz, L. A proposed spectral form for fully developed wind seas based on the similarity theory of S. A. Kitaigorodskii. *Journal of Geophysical Research* **1964**, *69*, 5181–5190. <https://doi.org/https://doi.org/10.1029/jz069i024p05181>. 582
583

62. Hasselann, K.; Al. Measurements of wind-wave growth and swell decay. *Ergänzungsheft zur Deutschen Hydrographischen Zeitschrift* **1973**, *12*. 584
585

63. Wu, G.; Hand, L.; Zhang, L. Numerical simulation and backscattering characteristics of freak waves based on JONSWAP spectrum. *Physical Oceanography* **2020**. <https://doi.org/https://doi.org/10.3389/fmars2020.585240>. 586
587

64. Guo, Q.; Xu, Z. Simulation of deep-water waves based on JONSWAP spectrum and realization by MATLAB. *19th International Conference on Geoinformatics* **2011**. <https://doi.org/https://doi.org/10.1109/geoinformatics.2011.5981100>. 588
589

65. Nishita, T.; Nakamae, E. Method of displaying optical effects within water using accumulation buffer. *SIGGRAPH'94* **1994**. <https://doi.org/https://doi.org/10.1145/192161.192261>. 590
591

66. Iwasaki, K.; Dobashi, Y.; Nishita, T. Efficient rendering of optical effects within water using graphics hardware. *Proceedings Ninth Pacific Conference on Computer Graphics and Applications* **2001**. <https://doi.org/https://doi.org/10.1109/pccga.2001.962894>. 592
593

67. Özgenel, F. Concrete crack images for classification. *Mendeley Data* **2019**, *2*. <https://doi.org/https://doi.org/10.17632/5y9wdsg2zt.2>. 594
595

68. V. Petruskiene, M.; Pal, Cao, M.; Jie, W.; Ragulskis, M. Color Recurrence Plots for Bearing Fault Diagnosis. *Sensors* **2022**, *22*. <https://doi.org/https://doi.org/10.3390/s22228870>. 596
597

Disclaimer/Publisher's Note: The statements, opinions and data contained in all publications are solely those of the individual author(s) and contributor(s) and not of MDPI and/or the editor(s). MDPI and/or the editor(s) disclaim responsibility for any injury to people or property resulting from any ideas, methods, instructions or products referred to in the content.

598
599
600